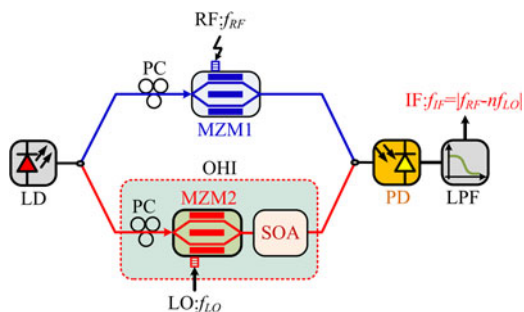


# Microwave Photonic Harmonic Down-Conversion Based on Cascaded Four-Wave Mixing in a Semiconductor Optical Amplifier

Volume 10, Number 1, February 2018

Xinhai Zou  
Shangjian Zhang, *Member, IEEE*  
Heng Wang  
Zhiyao Zhang  
Jinjin Li  
Yali Zhang  
Shuang Liu  
Yong Liu, *Senior Member, IEEE*



---

DOI: 10.1109/JPHOT.2017.2785409  
1943-0655 © 2017 IEEE

# Microwave Photonic Harmonic Down-Conversion Based on Cascaded Four-Wave Mixing in a Semiconductor Optical Amplifier

Xinhai Zou ,<sup>1</sup> Shangjian Zhang ,<sup>1</sup> Member, IEEE, Heng Wang ,<sup>1</sup>  
 Zhiyao Zhang,<sup>1</sup> Jinjin Li ,<sup>2</sup> Yali Zhang,<sup>1</sup> Shuang Liu,<sup>1</sup>  
 and Yong Liu,<sup>1</sup> Senior Member, IEEE

<sup>1</sup>Collaboration Innovation Center of Electronic Materials and Devices, State Key Laboratory of Electronic Thin Films and Integrated Devices, University of Electronic Science and Technology of China, Chengdu 610054, China

<sup>2</sup>Key Laboratory for Thin Film and Microfabrication of Ministry of Education, Department of Micro/Nano-electronics, Shanghai Jiao Tong University, Shanghai 200240, China

DOI: 10.1109/JPHOT.2017.2785409

1943-0655 © 2017 IEEE. Personal use is permitted, but republication/redistribution requires IEEE permission. See [http://www.ieee.org/publications\\_standards/publications/rights/index.html](http://www.ieee.org/publications_standards/publications/rights/index.html) for more information.

Manuscript received October 29, 2017; revised December 13, 2017; accepted December 15, 2017. Date of publication January 12, 2018; date of current version January 16, 2018. This work was supported in part by the NSFC of China under Grants 61377037, 61421002, 61435010, and 51672176, in part by the Innovation Funds of Collaboration Innovation Center of Electronic Materials and Devices under Grant ICEM2015-2001, in part by the Science Foundation for Youths of Sichuan Province under Grant 2016JQ0014), and in part by the Fundamental Research Funds for the Central Universities under Grant ZYGX2016J072. Corresponding author: Shangjian Zhang (e-mail: sjzhang@uestc.edu.cn).

**Abstract:** A reconfigurable and wideband photonic method is proposed for microwave photonic harmonic down-conversion based on cascaded four-wave mixing in a semiconductor optical amplifier (SOA). The cascaded four-wave mixing in SOA triggers high-order harmonics generation of local oscillator (LO) in the optical domain, and enables microwave down-conversion in the electrical domain with a low-frequency electrical LO. Compared with the conventional photonic method, ours allows microwave down-conversion operation for wide frequency range RF signal with a low-frequency electrical LO, and at the same time it avoids the requirement of complex phase control and heavy driving for the electrical LO. Moreover, it enables reconfigurable down-conversion with frequency tunability. In the demonstration, the 3~40 GHz RF signals are experimentally down-converted to IF signals below 2 GHz with a low-frequency electrical LO within the range of 5 GHz.

**Index Terms:** Microwave photonics, microwave harmonic down-conversion, cascaded four-wave mixing, optical harmonics intensification, semiconductor optical amplifier.

## 1. Introduction

The demands on great capacity and large instantaneous bandwidth have driven radio-frequency (RF) systems to operate at higher carrier frequency with wider signal bandwidth. Microwave down-conversion, as the essential functionality for the RF system, has attracted significant interest in wireless communication networks, phased-array antennas and electronic warfare systems [1]. However, conventional microwave mixers have limited bandwidth and low isolation, which cannot satisfy the requirements of high-frequency and wideband operation. In contrast, photonic-assisted techniques have been receiving intensive investigation in microwave down-conversion, thanks to the unique

advantages of large bandwidths, fast tunability, flexible configurability, high isolation, and immunity to electromagnetic interference [2].

The photonic-assisted schemes are mostly realized by electro-optical mixing between a RF signal and an electrical local oscillator (LO) through electro-optic modulators [3]–[6]. However, the operating frequency range is limited by the frequency range of the electrical LO and the bandwidth of the electro-optic modulators. In order to extend the operating frequency range of down-conversion, the microwave photonic harmonic down-conversion method has been proposed by using a mode-locked laser (MLL) [7], [8] or an optical frequency comb (OFC) [9]–[13]. The MLL-based method provides wide frequency range operation by the use of the evenly spaced optical carriers as the optical LO, however, the fixed repetition frequency of the MLL results in the poor frequency tunability of the achieved intermediate frequency (IF) signals [7]. The OFC-based method realizes reconfigurable harmonic down-conversion with tunable IF signals by adjusting the LO frequency. Nevertheless, the major limitation of OFC-based method when wide frequency range down-conversion is involved is the required heavy power driving [10]–[13] and/or precise phase control [12], [13] of the electrical LO signals (typical at around 30 dBm). Therefore, methods that allow reconfigurable and wide frequency range operation of microwave down-conversion, and avoid the need of high-frequency and high-power electrical LO are of great interest.

In this paper, we propose a photonic-assisted method based on cascaded four-wave mixing (CFWM) in a semiconductor optical amplifier (SOA), which enables reconfigurable and wide frequency range microwave down-conversion by using an electrical LO with low-frequency and power-efficiency. The proposed method consists of an electro-optic modulator and an optical harmonics intensifier (OHI) in a Mach-Zehnder interferometer (MZI). The CFWM in SOA triggers high-order harmonics generation of LO in the optical domain, and enables microwave down-conversion in the electrical domain with a low-frequency electrical LO. The proposed method can be operated with wide frequency range through high-order harmonic mixing between the RF and LO signals. Meanwhile, the microwave down-conversion can be reconfigured by adjusting the LO frequency. Therefore, the proposed harmonic down-conversion method is suitable for the single- and multiple-tone microwave signals. Compared with the conventional methods, ours here avoids the requirement of complex phase control and heavy power driving of electrical LO. In the experiment, the 3~40 GHz RF signals are down-converted to IF signals below 2 GHz with a low-frequency electrical LO (<5 GHz).

## 2. Theory Description

As is shown in Fig. 1, an optical carrier with the angular frequency of  $\omega_0 = 2\pi f_0$  is split into two arms of a MZI through an optical coupler. The optical carrier in the upper arm is modulated by a RF signal with the angular frequency of  $\omega_{RF} = 2\pi f_{RF}$  in a Mach-Zehnder modulator (MZM). The RF-modulated optical field can be expressed with Bessel function of the first kind as following [14]–[16]

$$\begin{aligned} E_{RF}(t) &= A_1 e^{j\omega_0 t} (e^{j\varphi_1} + \gamma_1 e^{jm_1 \sin \omega_{RF} t}) \\ &= A_1 \left[ e^{j\omega_0 t + j\varphi_1} + \gamma_1 \sum_{p=-\infty}^{+\infty} J_p(m_1) e^{j(\omega_0 + p\omega_{RF})t} \right], \end{aligned} \quad (1)$$

where  $A_1$  is the amplitude of the optical carrier in the upper arm.  $\varphi_1$  and  $\gamma_1$  are the phase bias and asymmetric factor of MZM1, respectively.  $m_1$  is the modulation index of MZM1 corresponding to the RF signal at the angular frequency of  $\omega_{RF}$ .

In the lower arm, the optical harmonics intensifier (OHI) consists of a MZM and an SOA. The optical carrier is firstly modulated by an electrical LO signal with the angular frequency of  $\omega_{LO} = 2\pi f_{LO}$  in the MZM2, which can be written by

$$E_{LO}(t) = A_2 e^{j\omega_0 t} (e^{j\varphi_2} + \gamma_2 e^{jm_2 \sin \omega_{LO} t}) = \sum_{q=-\infty}^{+\infty} B_q e^{j(\omega_0 + q\omega_{LO})t + j\xi_q}, \quad (2)$$

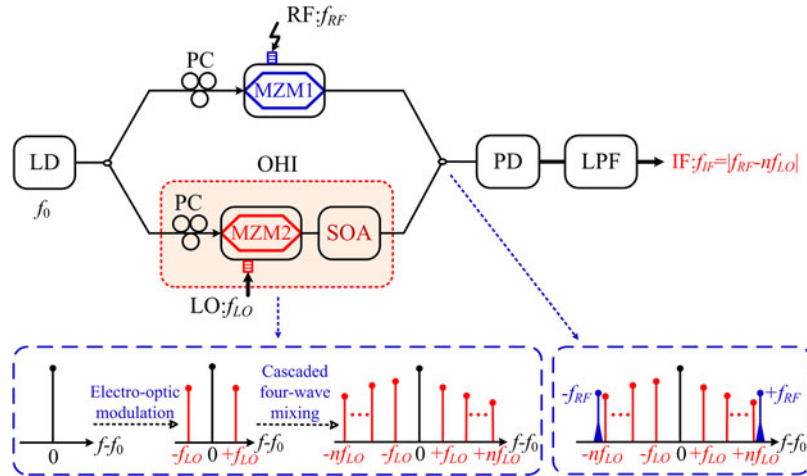


Fig. 1. Scheme of CFWM-based harmonic down-conversion with an SOA. LD, laser diode; PC, polarization controller; MZM, Mach-Zehnder modulator; OHI, optical harmonics intensifier; SOA, semiconductor optical amplifier; PD, photodetector; LPF, low-pass filter.

with the amplitude of the optical carrier  $A_2$  in the lower arm.  $\varphi_2$  and  $\gamma_2$  are the phase bias and asymmetric factor of MZM2, respectively.  $m_2$  is the modulation index of MZM2 corresponding to the electrical LO signal at the frequency of  $\omega_{LO}$ . For simplification,  $B_q$  and  $\xi_q$  are the amplitude and phase of the  $q$ th-order sideband, respectively.

The modulated optical signal from MZM2 is sent to an SOA, in which any two of the optical sidebands will generate new optical harmonic sidebands through FWM effect of SOA. The newly formed sidebands can in turn interact with each other to further generate new higher-order ones through FWM, involving a cascaded process known as CFWM. The new  $n$ th-order optical harmonic sideband can be written as [17]

$$\begin{aligned} E'_n(t) &= B_n e^{j(\omega_0+n\omega_{LO})t+j\xi_n} + \sum_{p=-\infty}^{+\infty} \chi(\Delta\omega_{pq}) \left[ B_p e^{j(\omega_0+p\omega_{LO})t+j\xi_p} \right] \\ &\quad \times \left[ B_q e^{j(\omega_0+q\omega_{LO})t+j\xi_q} \right]^* \left[ B_p e^{j(\omega_0+p\omega_{LO})t+j\xi_p} \right] \\ &= \left[ B_n e^{j\xi_n} + \sum_{p=-\infty}^{+\infty} \chi(\Delta\omega_{pq}) B_p^2 B_q e^{j(2\xi_p-\xi_q)} \right] \cdot e^{j(\omega_0+n\omega_{LO})t}, \quad q = 2p - n \end{aligned} \quad (3)$$

where  $\chi(\Delta\omega_{pq})$  is the relative conversion efficiency of the FWM effect and inversely proportional to  $\Delta\omega_{pq}$  ( $\Delta\omega_{pq} = (p - q)^*\omega_{LO}$ ,  $|p| \geq |q|$ ). We assume the intensified optical harmonic signal from OHI can be simplified as [18]

$$E_{OHI}(t) = \sum_{n=-N_1}^{+N_2} E'_n(t) = \sum_{n=-N_1}^{+N_2} F_n e^{j(\omega_0+n\omega_{LO})t+j\phi_n}, \quad (4)$$

where  $F_n$  and  $\phi_n$  are the amplitude and phase of the new  $n$ th-order sideband, respectively.  $N_1$  and  $N_2$  correspond to the maximum lower and upper sideband with respect to the optical carrier, respectively.

The optical signals in the two arms of MZI are combined through the second optical coupler, and then detected by a photodetector (PD) to generate a photocurrent, which can be written as

$$i(t) = R \cdot [E_{RF}(t) e^{j\theta} + E_{OHI}(t)] [E_{RF}(t) e^{j\theta} + E_{OHI}(t)]^*, \quad (5)$$

with the PD responsivity  $R$  and the phase difference  $\theta$  between the two arms of MZI.

After photodetection, the mixing signals at  $\omega_{IF} = |p\omega_{RF} - n\omega_{LO}|$  are produced by the optical beating between the RF-modulated optical sidebands in the upper arm of MZI and the CFWM-generated  $n$ th-order harmonic sidebands in the lower arm of MZI, which can be expressed as

$$i_{MIX}(t) = \sum_{n=-N_1}^{+N_2} \sum_{p=-\infty}^{+\infty} 2\gamma_1 A_1 F_n J_p(m_1) R(\omega_{IF}) \cos[(p\omega_{RF} - n\omega_{LO})t + \theta - \phi_n]. \quad (6)$$

In the case of down-conversion, the desired IF signal at  $\omega_{IF} = |\omega_{RF} - n\omega_{LO}|$  (i.e.,  $p = \pm 1$ ) is achieved after an electrical low-pass filter (LPF) as following

$$i_{IF}(t) = 2\gamma_1 A_1 \alpha J_1(m_1) R(\omega_{IF}) \cos(|\omega_{RF} - n\omega_{LO}|t + \psi), \quad (7)$$

with the magnitude and phase coefficients  $\alpha$  and  $\psi$  of the down-converted IF signal

$$\alpha = \sqrt{F_n^2 + F_{-n}^2 - 2F_n F_{-n} \cos(2\theta - \phi_n - \phi_{-n})} \quad (8)$$

$$\psi = \arctan \left[ \frac{F_n \sin(\theta - \phi_n) + F_{-n} \sin(\theta - \phi_{-n})}{F_n \cos(\theta - \phi_n) - F_{-n} \cos(\theta - \phi_{-n})} \right]. \quad (9)$$

From (7), the proposed method can be operated with a frequency range of  $(\text{Max}(N_1, N_2) + 0.5)*\omega_{LO}$ , which is proportional to the highest order of optical harmonic sidebands of the LO. Thus, microwave down-conversion can be achieved with wide frequency range by using different order optical harmonic tones of the same low-frequency LO. Moreover, the converted IF signal can be configured by adjusting the LO frequency. From (3), the high-order harmonic sidebands are generated through the CFWM of SOA, which avoids the requirement of complex phase control and heavy power driving of the LO.

### 3. Experiment and Results

In the experiment, the optical carrier comes from a DFB laser diode with a wavelength of 1550.13 nm and an optical power of 10.87 dBm, which is split into two arms of MZI through an optical coupler. The optical carrier in the upper arm of MZI is sent to LiNbO<sub>3</sub> MZM (MZM1, Sumitomo T-DKH1.5) and modulated by an RF signal at the frequency of  $\omega_{RF}$  from a microwave source (R&S SMA 100A). The optical carrier in the lower arm of MZI is sent to the OHI consisting of a MZM (MZM2, EOspace AX-OMSS-20) and an SOA (Kamelian SOA-NL) with a small-signal gain of 26 dB@1550 nm, a 3 dB bandwidth of 43 nm and a gain recovery time of 25 ps in the case of 200 mA injection current. The MZM2 is driven by an electrical LO signal at the frequency of  $\omega_{LO}$  from another microwave source (R&S SMA 100A). Then, the modulated optical signal from MZM2 is sent to the SOA to trigger optical harmonics generation based on CFWM effect. The optical signals from the two arms are combined through an optical coupler and detected by a photodetector (PD, HP 11982A) and an electrical LPF to obtain the down-converted IF signal. In order to minimize the environmental impact on the output signal of MZI, the optical paths of MZI are close to each other and the MZI is fixed on the optical table.

In our demonstration, the electrical LO is set at the frequency of 4.88 GHz with the microwave power of 10 dBm and applied to the MZM2 with the bias voltage of 7.45 V and the modulation index of 0.445 [19]. The input power of the SOA is -4.14 dBm. Fig. 2 shows the optical spectra after the OHI, in the cases of the SOA biased at different currents. When the SOA is biased at 20 mA and operated in linear range, the output spectrum of OHI is similar to the optical spectrum of the LO-modulated optical signal used for triggering high-order harmonic generation in the OHI. The number of the harmonic sidebands increases with the injection current of SOA because of the CFWM effect in the SOA. For example, there are 3, 5, 7, and 9 harmonic sidebands in the 10 dB reduction bandwidth when the SOA is biased at 50 mA, 100 mA, 200 mA and 300 mA, respectively. Therefore, the high-order harmonic sidebands can be configured by setting the injection current of SOA, which verifies the elimination of complex phase control and heavy power driving of the LO for high-order harmonics generation. The generated harmonic sidebands number is different on each

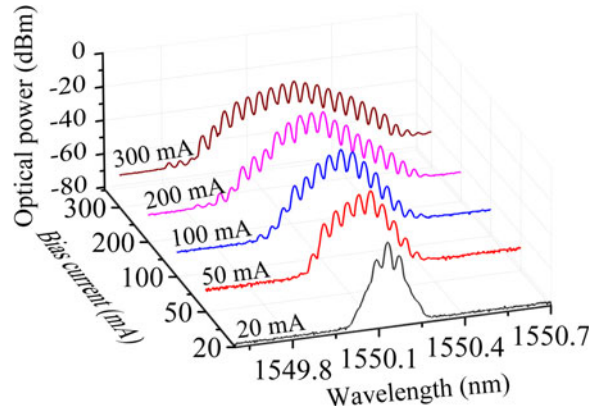


Fig. 2. Measured optical spectra of OHI when the SOA is biased at different currents.

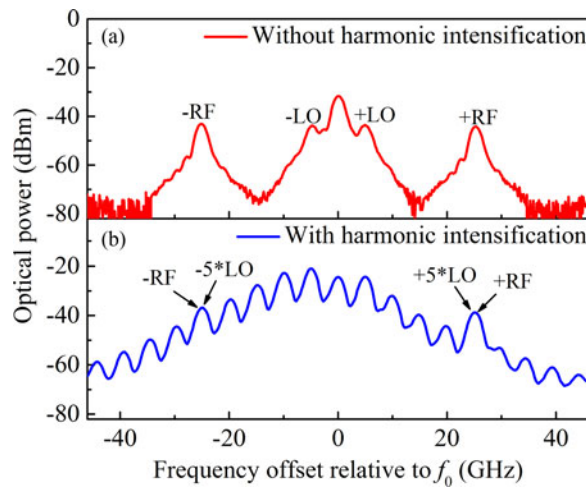


Fig. 3. Optical spectra before photodetection when  $f_{RF} = 25$  GHz and  $f_{LO} = 4.88$  GHz, in the cases of (a) without harmonic intensification and (b) with harmonic intensification.

side of the optical carrier and the amplitude is also different for the same order harmonic sidebands, which results from the asymmetric conversion efficiency of FWM. From (7) and (8), the power of IF signal will be influenced by the asymmetric amplitude, in which the impact can be minimized by adjusting the bias phase of MZM1 and/or MZM2. Moreover, the asymmetric comb by CFWM will be helpful to operation frequency range of down-conversion due to the higher-order harmonic sidebands generation on one side of optical carrier.

Fig. 3 illustrates the optical spectra from the MZI when the RF signal is set at the frequency of 25 GHz with the microwave power of 10 dBm. In the case of without the harmonic intensification, the optical spectra include the first-order sidebands of RF- and LO-modulated optical signal, while there are several high-order sidebands of LO generated near the first-order sidebands of RF in the case of with the harmonic intensification based on the CFWM effect in an SOA.

When the SOA is biased at 200 mA, the output power of SOA is 11.83 dBm and the received power of PD is 9.35 dBm. The 25-GHz RF signal is down-converted through the fifth-order harmonics of LO to the IF frequency at  $f_{IF} = |25 - 5 * 4.88|$  GHz = 0.6 GHz with the signal-to-noise ratio (SNR) of 43.38 dB, as shown in Fig. 4. The conversion efficiency without electrical amplify is determined to be  $-35.04$  dB, which is defined as the electrical power ratio between the converted IF signal and the RF signal. The conversion efficiency can be improved by selecting the desired optical signal with an optical filter before photodetection and cascading SOAs or replacing the SOA with higher nonlinear

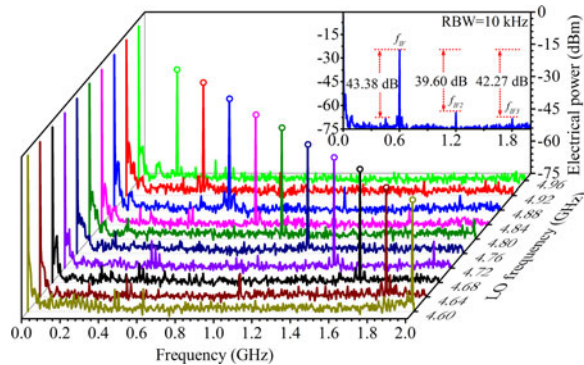


Fig. 4. Measured electrical spectra of the IF signals converted from the same 25-GHz RF signal while the electrical LO frequency is tuning from 4.96 GHz to 4.6 GHz, where the inset shows the 0.6-GHz IF signal spectrum line.

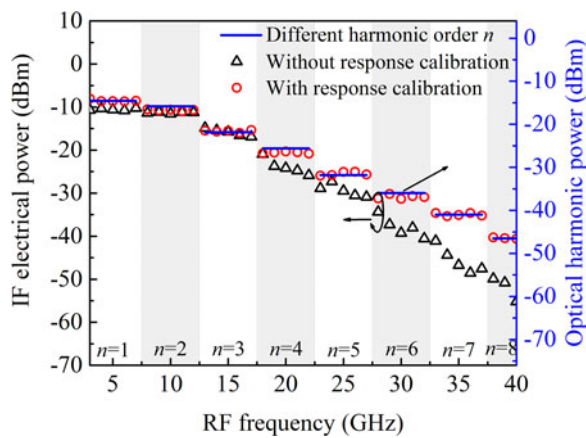


Fig. 5. Electrical power of IF signals when the 3~40 GHz RF signals are converted to IF signals within 2 GHz through different order harmonic sidebands, in the cases of without and with calibrating the frequency response of MZM1 for different RF signals, and the optical power of the first-order to eighth-order harmonic sidebands.

material, such as  $\text{As}_2\text{S}_3$  [20]. There are also parasitic signals observed at  $f_{IF2} = |2 * 25 - 10 * 4.88| \text{GHz} = 1.2 \text{GHz}$  and  $f_{IF3} = |3 * 25 - 15 * 4.88| \text{GHz} = 1.8 \text{GHz}$  with spur suppression ratio of 39.60 dB and 42.27 dB, respectively. The 25-GHz RF signal can be also down-converted to different IF signals below 2 GHz by tuning the electrical LO frequency from 4.96 GHz to 4.6 GHz, as shown in Fig. 4, allowing flexible down-conversion for wideband RF signals. All the down-converted IF signals show extremely narrow spectrum lines due to the inherent coherence of the RF-modulated and LO-modulated sidebands in the MZI originating from the same optical carrier [21]–[23]. Besides, for an unknown RF signal, the RF frequency can be determined by analyzing three beat tones between the RF signal and the nearest harmonic sideband in the case of setting different LO frequencies [24].

To extend the operation frequency range, different bands of RF signals can be down-converted to IF band with the same LO by using different order harmonic down-conversion. As the triangle symbols shown in Fig. 5, different RF signals ranging from 3 to 40 GHz are converted to the IF signal within 2 GHz by using the first-order to eighth-order harmonics down-conversion in the case of the LO frequency  $f_{LO} = 4.88 \text{GHz}$ . The electrical power of converted IF signal decreases with the increase of RF frequency. From (7) and (8), the decreasing electrical power of converted IF signal is attributed to the degraded efficiency of the MZM1 for RF modulation and the OHI for high-order harmonics generation. To prove this, we keep a constant modulation depth of MZM1 for different

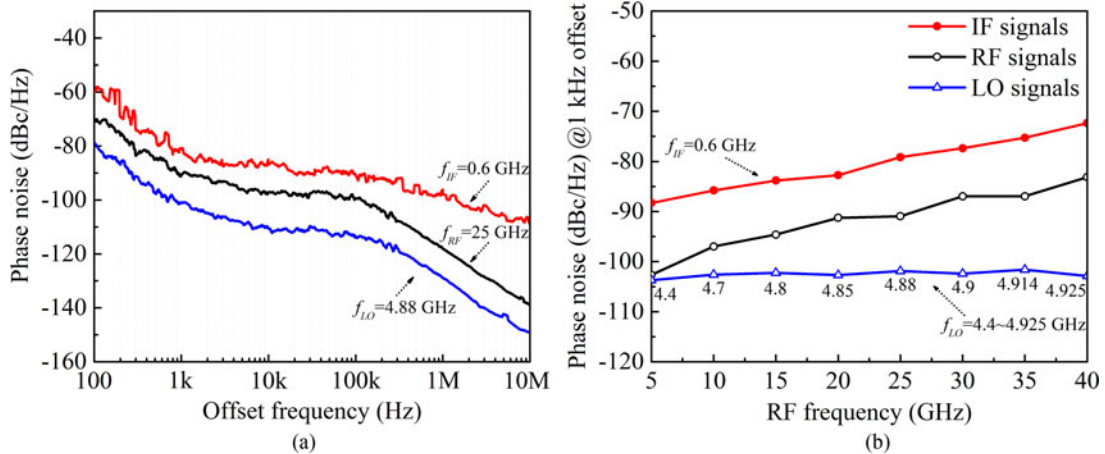


Fig. 6. Measured phase noises (a) in the case of  $f_{RF} = 25 \text{ GHz}$ ,  $f_{LO} = 4.88 \text{ GHz}$  and  $f_{IF} = 0.6 \text{ GHz}$ , and (b) at the 1 kHz offset in the case of  $f_{RF} = 5 \sim 40 \text{ GHz}$ ,  $f_{LO} = 4.4 \sim 4.925 \text{ GHz}$  and  $f_{IF} = 0.6 \text{ GHz}$ .

RF signals down-conversion, in which the degraded response of the MZM1 is calibrated. As shown in Fig. 5, the performance of down-conversion is improved after response calibration. In practice, a wideband MZM1 with flat response will be helpful to the down-conversion performance. As the circular symbols and solid line shown in Fig. 5, it can be observed that the power of converted IF signals show very similar variation with that of the generated harmonic sidebands. The operating frequency range of down-conversion can be further extended through increasing the number and space of the harmonic tones by optimizing the frequency of electrical LO and the CFWM of SOA.

We also evaluate the phase noise performance of the generated IF signals. As shown in Fig. 6(a), the phase noise of the RF, LO and IF signal are measured in the conversion from a 25-GHz RF signal to 0.6-GHz IF signal with 4.88-GHz LO signal. The generated 0.6-GHz IF signal has a phase noise as low as  $-80.02 \text{ dBc/Hz}$  at an offset frequency of 1 kHz. Compared with the RF signal, the LO signal features at least 10 dB lower phase noise while the IF signal has more than 6 dB higher phase noise in the offset frequency range of 100 Hz to 10 MHz. To investigate the dependence of the phase noise, we measure the phase noise of the RF, LO and IF signal at the offset frequency of 1 kHz when the down-conversion is operated from 5 GHz–40 GHz RF signals to the 0.6-GHz IF signals by tuning the electrical LO frequency, as shown in Fig. 6(b). The phase noise of the LO signals has a negligible fluctuations, however, the phase noise of the RF and IF signals are both degraded with the increase of RF frequency and have a similar variation tendency. Therefore, the phase noise of the IF signal is mainly resulted from the degraded phase noise of the RF signal in our experiment. When the offset frequency is higher than 100 kHz, the IF phase noise is mainly contributed by the residual phase noise of the system [25], including amplified spontaneous emission (ASE) noise of SOA, that is why, the phase noise slopes of both IF and RF signal are a little bit different in the offset frequency range of 100 kHz to 10 MHz.

#### 4. Conclusion

We have proposed a CFWM-based photonics method for reconfigurable and wideband microwave harmonic down-conversion with a low-frequency electrical LO. In the demonstration, RF signals ranging from 3 to 40 GHz are down-converted to the IF signals within 2 GHz with a 5-GHz LO. Compared with the conventional electro-optical mixing approach, the proposed method enables wide frequency range microwave down-conversion with a low-frequency electrical LO. Unlike the competing OFC-based harmonic down-conversion method, our method avoids the requirement of complex phase control and heavy power driving for the electrical LO, and at the same time it enables reconfigurable and wideband harmonic down-conversion by tuning a low-frequency electrical LO.

## References

- [1] J. P. Yao, "Microwave photonics," *J. Lightw. Technol.*, vol. 27, no. 3, pp. 314–335, Feb. 2009.
- [2] J. Capmany and D. Novak, "Microwave photonics combines two worlds," *Nature Photon.*, vol. 1, no. 6, pp. 319–330, Jun. 2007.
- [3] P. X. Li, W. Pan, X. H. Zou, S. L. Pan, B. Luo, and L. S. Yan, "High-efficiency photonic microwave downconversion with full-frequency-range coverage," *IEEE Photon. J.*, vol. 7, no. 4, Aug. 2015, Art. no. 5500907.
- [4] Z. Z. Tang and S. L. Pan, "A reconfigurable photonic microwave mixer using a 90° optical hybrid," *IEEE Trans. Microw. Theory Tech.*, vol. 64, no. 9, pp. 3017–3025, Sep. 2016.
- [5] Y. S. Gao, A. J. Wen, Z. Y. Tu, W. Zhang, and L. Lin, "Simultaneously photonic frequency downconversion, multichannel phase shifting, and IQ demodulation for wideband microwave signals," *Opt. Lett.*, vol. 41, no. 19, pp. 4484–4487, Oct. 2016.
- [6] S. Hughes *et al.*, "Agile micro- and millimeter-wave communication using photonic frequency conversion," in *Proc. Opt. Fiber Commun. Conf.*, Mar. 2016, pp. 1–3.
- [7] J. X. Liao, X. P. Zheng, S. Y. Li, H. Y. Zhang, and B. K. Zhou, "High-efficiency microwave photonic harmonic down-conversion with tunable and reconfigurable filtering," *Opt. Lett.*, vol. 39, no. 23, pp. 6565–6568, Dec. 2014.
- [8] F. Scotti, F. Laghezza, P. Ghelfi, S. Pinna, G. Serafino, and A. Bogoni, "Photonic-based RF transceiver for UWB multi-carrier wireless systems," *Photonics*, vol. 1, no. 2, pp. 146–153, May 2014.
- [9] M. G. Wang and J. P. Yao, "Tunable optical frequency comb generation based on an optoelectronic oscillator," *IEEE Photon. Technol. Lett.*, vol. 25, no. 21, pp. 2035–2038, Nov. 2013.
- [10] V. R. Pagán and T. E. Murphy, "Electro-optic millimeter-wave harmonic downconversion and vector demodulation using cascaded phase modulation and optical filtering," *Opt. Lett.*, vol. 40, no. 11, pp. 2481–2484, Jun. 2015.
- [11] X. W. Yang *et al.*, "Optical frequency comb based multi-band microwave frequency conversion for satellite applications," *Opt. Exp.*, vol. 22, no. 1, pp. 869–877, Jan. 2014.
- [12] T. Zhang *et al.*, "High-spectral-efficiency photonic frequency down-conversion using optical frequency comb and SSB modulation," *IEEE Photon. J.*, vol. 5, no. 2, Apr. 2013, Art. no. 7200307.
- [13] X. Fang, M. Bai, X. Z. Ye, J. G. Miao, and Z. Zheng, "Ultra-broadband microwave frequency down-conversion based on optical frequency comb," *Opt. Exp.*, vol. 23, no. 13, pp. 17111–17119, Jun. 2015.
- [14] S. J. Zhang, H. Wang, X. H. Zou, Y. L. Zhang, R. G. Lu, and Y. Liu, "Calibration-free electrical spectrum analysis for microwave characterization of optical phase modulators using frequency-shifted heterodyning," *IEEE Photon. J.*, vol. 6, no. 4, Aug. 2014, Art. no. 5501008.
- [15] S. J. Zhang, C. Zhang, H. Wang, X. H. Zou, Y. Liu, and J. E. Bowers, "Calibration-free measurement of high-speed Mach-Zehnder modulator based on low-frequency detection," *Opt. Lett.*, vol. 41, no. 3, pp. 460–463, Feb. 2016.
- [16] H. Wang *et al.*, "Self-calibrated and extinction-ratio-independent microwave characterization of electrooptic Mach-Zehnder modulators," *IEEE Microw. Wireless Compon. Lett.*, vol. 27, no. 10, pp. 948–950, Oct. 2017.
- [17] J. X. Ma *et al.*, "Wavelength conversion based on four-wave mixing in high-nonlinear dispersion shifted fiber using a dual-pump configuration," *J. Lightw. Technol.*, vol. 24, no. 7, pp. 2851–2858, Jul. 2006.
- [18] Z. Tong, A. O. J. Wiberg, E. Myslivets, B. P. P. Kuo, N. Alic, and S. Radic, "Spectral linewidth preservation in parametric frequency combs seeded by dual pumps," *Opt. Exp.*, vol. 20, no. 16, pp. 17610–17619, Jul. 2012.
- [19] S. J. Zhang *et al.*, "Self-calibrated microwave characterization of high-speed optoelectronic devices by heterodyne spectrum mapping," *J. Lightw. Technol.*, vol. 35, no. 10, pp. 1952–1961, May 2017.
- [20] M. D. Pelusi *et al.*, "Ultra-high nonlinear As<sub>2</sub>S<sub>3</sub> planar waveguide for 160-Gb/s optical time-division demultiplexing by four-wave mixing," *IEEE Photon. Technol. Lett.*, vol. 19, no. 19, pp. 1496–1498, Oct. 2007.
- [21] S. J. Zhang, H. Wang, X. H. Zou, Y. L. Zhang, R. G. Lu, and Y. Liu, "Self-calibrating measurement of high-speed electro-optic phase modulators based on two-tone modulation," *Opt. Lett.*, vol. 39, no. 12, pp. 3504–3507, Jun. 2014.
- [22] S. J. Zhang, H. Wang, X. H. Zou, Y. L. Zhang, R. G. Lu, and Y. Liu, "Extinction-ratio-independent electrical method for measuring chirp parameters of Mach-Zehnder modulators using frequency-shifted heterodyne," *Opt. Lett.*, vol. 40, no. 12, pp. 2854–2857, Jun. 2015.
- [23] S. J. Zhang, C. Zhang, H. Wang, Y. Liu, J. D. Peters, and J. E. Bowers, "On-wafer probing-kit for RF characterization of silicon photonic integrated transceivers," *Opt. Exp.*, vol. 25, no. 12, pp. 13340–13350, Jun. 2017.
- [24] Y. X. Ma *et al.*, "Broadband high-resolution microwave frequency measurement based on low-speed photonic analog-to-digital converters," *Opt. Exp.*, vol. 25, no. 3, pp. 2355–2368, Feb. 2017.
- [25] W. Z. Li and J. P. Yao, "Investigation of photonically assisted microwave frequency multiplication based on external modulation," *IEEE Trans. Microw. Theory Tech.*, vol. 58, no. 11, pp. 3259–3268, Nov. 2010.